Journal of Alloys and Compounds 509S (2011) S679–S683

Contents lists available at ScienceDirect

Journal of Alloys and Compounds

journal homepage: www.elsevier.com/locate/jallcom

A computational study on the effect of fluorine substitution in $LiBH_4$

Marta Corno, Eugenio Pinatel, Piero Ugliengo, Marcello Baricco*

Dipartimento di Chimica I.F.M. and NIS, Università di Torino, via Giuria 7/9, 10125 Torino, Italy

ARTICLE INFO

Article history:
Received 4 August 2010
Received in revised form
24 September 2010
Accepted 4 October 2010
Available online 10 October 2010

Keywords:
Hydrogen storage material
Metal hydride
Thermodynamic properties
Computer simulation

ABSTRACT

Hydrogen substitution by fluorine in the orthorhombic phase of $LiBH_4$ has been investigated with quantum-mechanics calculations aiming at describing thermodynamic properties of $LiB(H,F)_4$ solid solutions for hydrogen storage applications. Excess enthalpy of the mixed compounds was computed with the periodic *ab initio* CRYSTAL09 code, within the density functional approach and localised Gaussian basis sets, and used for Calphad thermodynamic modelling. The large number of possible mixed configurations for a given fluorine content were reduced by symmetry equivalence criteria. Deep analysis of the results highlights the relevance of structures in which, for a given H/F ratio, fluorine ions are likely to belong to the same BH_4 tetrahedron, rather than be dispersed over the available tetrahedra. This "locality principle" dramatically reduced the configurational space to be explored by expensive quantum-mechanical calculations. Our data show that, at room temperature, the formation of solid solutions between lithium borohydride and borofluoride is not thermodynamically favoured, so that the fluorine substitution destabilizes the pure hydride.

1. Introduction

Recently, hydrogen storage materials have been widely investigated in order to obtain high volumetric and gravimetric hydrogen density for safe and efficient onboard applications [1]. Among the various methods to store hydrogen, solid metal–hydrogen compounds are currently being considered due to their very promising properties. Particularly, complex hydrides of aluminium and boron with alkali, alkali earth and transition metals form a large number of lightweight metal–hydrogen compounds. The main advantage of these complex hydrides is represented by their high gravimetric density, e.g. for $LiBH_4$ at room temperature equal to 18 mass%. Unfortunately, they are also well-known to exhibit a high thermal stability and unfavourable hydrogen absorption and desorption kinetics [2,3]. To overcome these drawbacks, several strategies have been applied, such as the combination with metal hydrides [4], the partial cation substitution [5], the confinement in nanoporous scaffolds [6]. Among these, anion substitution is one of the possible routes for the synthesis of new mixed material with tuneable thermodynamic properties [7]. Specifically, mixing borohydrides and halides of the same metal exploits the higher electronegativity of the halogen, changing the bond strength of the remaining components. Thus, release and possibly uptake of hydrogen can be facilitated [8,9].

Among classical experimental techniques, computational methods are increasingly being applied in the research field of hydrogen storage materials [10], both to predict the formation of new phases or compounds [11] and to complement the difficult interpretation of experimental characterization [12]. Considering anion substitutions, *ab initio* calculations were used to study thermodynamics properties of decomposition reactions of $NaAlH_4$ [13], $LiBH_4$ [14] as well as $Ca(BH_4)_2$ [15] mixed with different halides. Nevertheless, much information is still lacking and the synergetic contribution of experimental and theoretical methods represents a fundamental tool to a deeper understanding of these mechanisms.

In the present paper, we describe a computational approach towards the description of the formation reaction of solid solutions between $LiBH_4$ and $LiBF_4$ at room temperature using density functional theory (DFT) calculations, in order to state whether the fluorine effect is to stabilize or destabilize the pure borohydride.

2. Computational methods

Ab initio calculations based on DFT GGA Hamiltonian (PBE[16]) were carried out with the periodic CRYSTAL09 [17,18] code and localized basis set functions of polarized double-ζ quality. In details, Li cation was described with a 5-11G(d) basis set [19] ($\alpha_{sp} = 0.479\ bohr^{-2}$ for the most diffuse shell exponent and $\alpha_{pol} = 0.600\ bohr^{-2}$ for polarization), while for boron a 6-21G(d) [20] ($\alpha_{sp} = 0.124\ bohr^{-2}$ for the most diffuse shell exponent and $\alpha_{pol} = 0.800\ bohr^{-2}$ for polarization) was adopted. For hydrogen and

* Corresponding author at: via P. Giuria 9, 10125 Torino, Italy. Tel.: +39 011 6707569; fax: +39 011 6707856.
E-mail addresses: marta.corno@unito.it (M. Corno), eugenio.pinatel@unito.it (E. Pinatel), piero.ugliengo@unito.it (P. Ugliengo), marcello.baricco@unito.it (M. Baricco).

0925-8388/$ – see front matter © 2010 Elsevier B.V. All rights reserved.
doi:10.1016/j.jallcom.2010.10.005

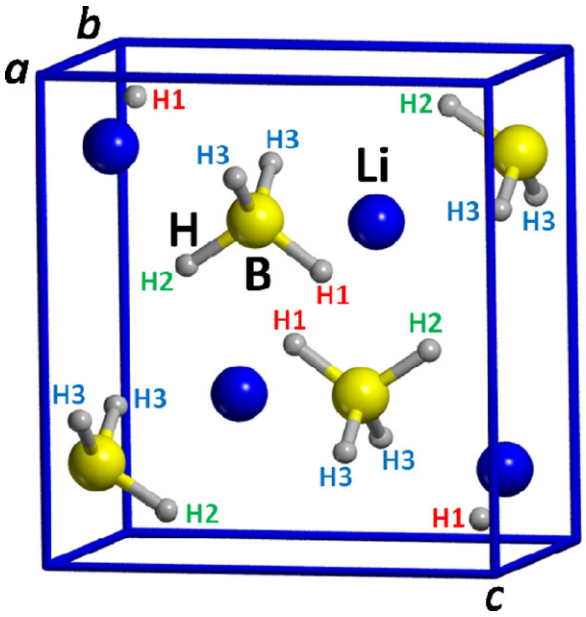

Fig. 1. Orthorhombic *Pnma* $LiBH_4$ optimized unit cell; hydrogen labeled in terms of symmetry equivalence (color coding: Li blue, B yellow, H light grey, cell borders in blue).(For interpretation of the references to colour in this figure legend, the reader is referred to the web version of the article.)

fluorine a 31G(p) [21] (α_{sp} = 0.1613 bohr^{-2} for the most diffuse shell exponent and α_{pol} = 1.1 bohr^{-2} for polarization) and a 7-311G(d) [22] were considered, respectively.

Phonons at Γ point in the harmonic approximation were computed to derive the thermodynamic functions by diagonalizing the associated mass-weighted Hessian matrix (for details on the computational procedure see references [23,24]).

The enthalpy data were obtained as the electronic energy including the zero-point energy correction (ZPE) and the thermal factor at T = 298K. As for entropy, two contributions were evaluated, *i.e.* the *configurational entropy*, deriving from the number of possible symmetry equivalent configurations with the same degree of fluorine substitution inside the unit cell and the *thermal entropy*, computed from frequency values for a given configuration. The resulting enthalpy was used to work out the excess enthalpy as a function of F content, which is the main focus of this note. Thermodynamic calculations using the *ab initio* results were carried out with the Thermocalc software [25].

3. Results and discussion

Low-temperature pure orthorhombic $LiBH_4$ (*Pnma* space group) has been fully optimized starting from the experimental structural data of Hartman et al. [26]. Table 1 reports experimental and PBE simulated lattice parameters and bond lengths of the BH_4 tetrahedron, labelled as in Fig. 1 and according to reference [26]. Fig. 1 shows the optimized unit cell containing 24 atoms, that is four equivalent tetrahedra (Z = 4) corresponding to 16 hydrogen. Comparison between PBE and experiment reveals a systematic enlargement of the B–H distances, by approximately 0.16 Å on the averaged value. IR spectrum was computed in the harmonic approximation and the obtained frequencies belong to the following ranges: 2294–2490 cm^{-1} for B–H stretching (most intense peak at 2389 cm^{-1}) and 990–1350 cm^{-1} for H–B–H bending (most intense peak at 1244 cm^{-1}). The punctual comparison with available experimental data is out of the scope of the present article and will be addressed in a future work.

The pure $LiBF_4$ was optimized within the trigonal phase ($P3_121$ space group [27]), which is the most stable phase at room temperature. Nevertheless, our approach was to compute $LiBF_4$ within an orthorhombic lattice (*Pnma* space group) to avoid phase transition modelling. Table 1 summarizes both trigonal and orthorhombic structural features, compared to experimental data for the trigonal phase. Actually, the geometry optimization process led to very similar bond lengths in both cases (averaged values for trigonal and orthorhombic structures: 1.421 and 1.420 Å, respectively). The optimized trigonal structure was proven to be 5.8 kJ mol^{-1} per formula unit more stable than the optimized orthorhombic, as expected.

In order to model solid solutions between $LiBH_4$ and $LiBF_4$, the adopted procedure contemplates the following steps: (i) classifi-

Table 1
Lattice parameters and most relevant bond lengths for optimized DFT models of orthorhombic $LiBH_4$, trigonal $LiBF_4$ and orthorhombic $LiBF_4$, compared to the corresponding available experimental values. All data expressed in Å. H and F labels refer to Fig. 1.

$LiBH_4$ *Pnma*	*a*	*b*	*c*	B-H1	B-H2	B-H3	Average B-H
Exp.*	7.121	4.406	6.674	1.213	1.224	1.208	1.215
DFT	7.328	4.379	6.494	1.230	1.233	1.229	1.231
$LiBF_4$	*a*	*b*	*c*	B-F1	B-F2	B-F3	Average B-F
Exp. $P3_121$**	4.892	4.892	11.002	1.387	1.391	–	1.389
DFT $P3_121$	4.960	4.960	11.173	1.421	1.422	–	1.421
DFT *Pnma*	7.409	5.477	8.961	1.418	1.420	1.421	1.420

* Reference [26].
** Reference [27].

Table 2
Total number of possible $LiBH_{16-a}F_a$ configurations (fourth column) for each composition a (second column, $1 \le a \le 8$) and molar fraction of $LiBF_4x$ (third column) corresponding to a specific formula unit (first column) and organization in symmetry non equivalent classes (last column).

Formula unit	*a*	*x*	Total number of configurations	Number of different classes
$LiBH_{3.75}F_{0.25}$	1	0.062	16	3
$LiBH_{3.5}F_{0.5}$	2	0.125	120	25
$LiBH_{3.25}F_{0.75}$	3	0.187	560	81
$LiBH_3F_1$	4	0.250	1820	272
$LiBH_{2.75}F_{1.25}$	5	0.312	4368	587
$LiBH_{2.5}F_{1.5}$	6	0.375	8008	1103
$LiBH_{2.25}F_{1.75}$	7	0.437	11440	1505
$LiBH_2F_2$	8	0.500	12870	1742

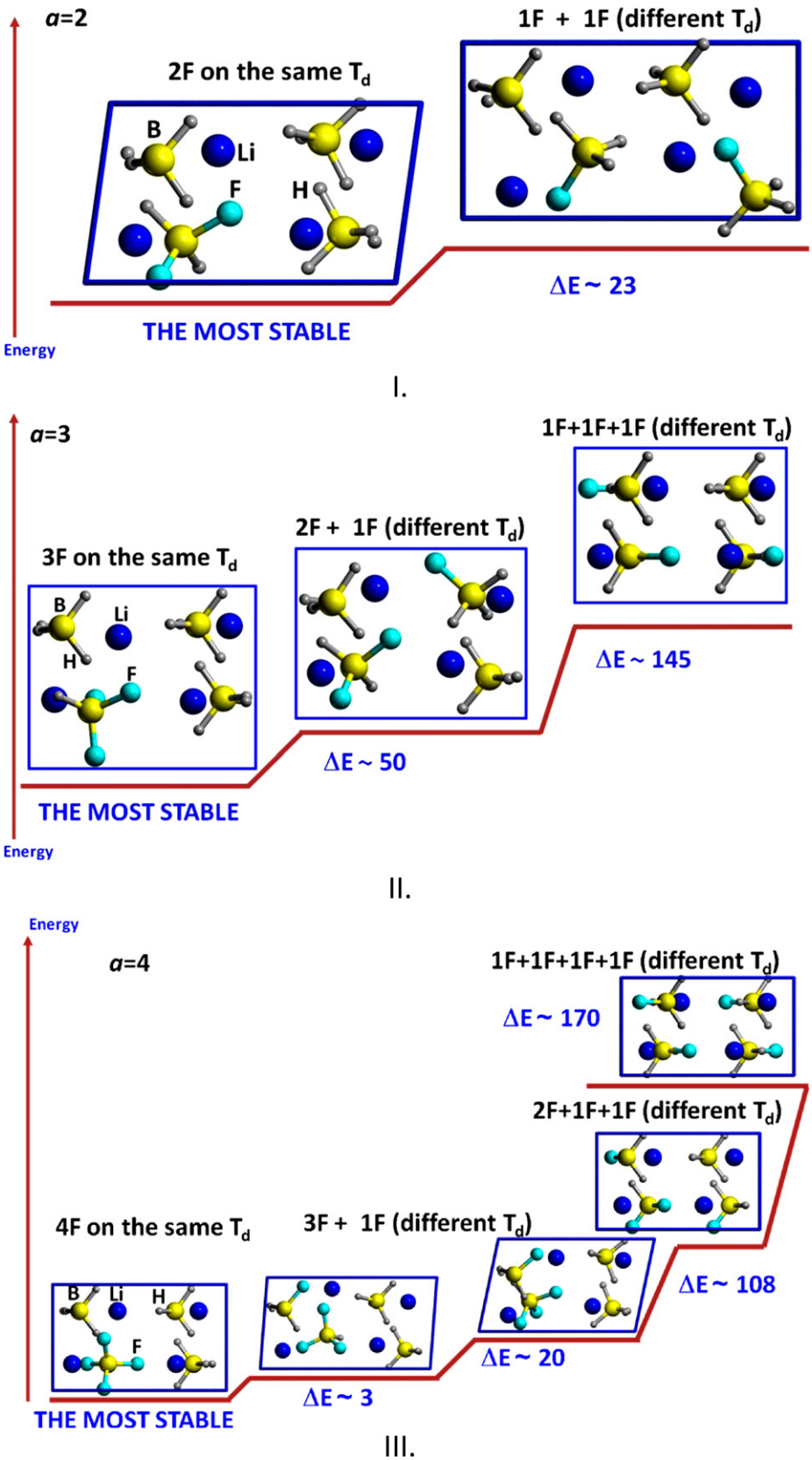

Fig. 2. Graphical examples of the "locality principle": I. for $LiBH_{3.5}F_{0.5}$ ($a=2$), II. $LiBH_{3.25}F_{0.75}$ ($a=3$) and III. $LiBH_3F_1$ ($a=4$). Reported ΔE values are based on electronic energy calculations (no ZPE included) and expressed as relative energy in kJ mol^{-1} with respect to the most stable optimized structure for each composition, normalized to the formula unit. T_d indicates tetrahedron/(a). Color coding: Li blue, B yellow, H light grey, F light blue, cell borders in blue.(For interpretation of the references to colour in this figure legend, the reader is referred to the web version of the article.)

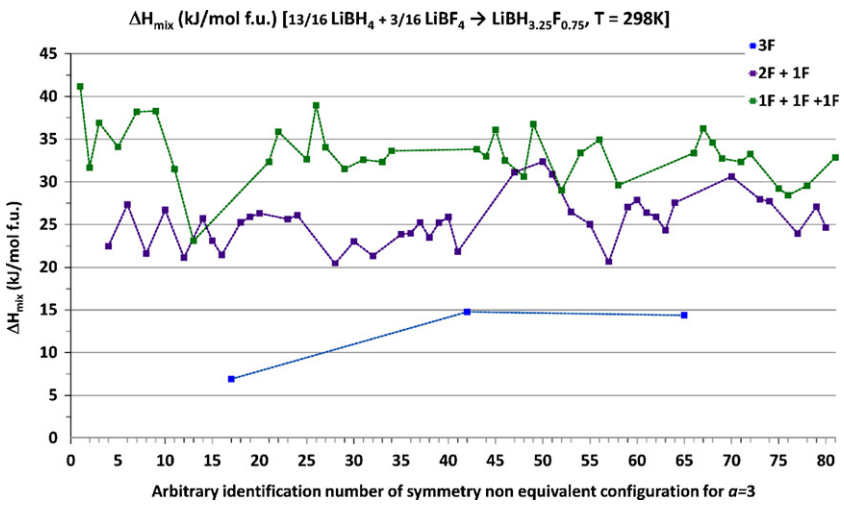

Fig. 3. Enthalpy of mixing for the reaction of formation of $LiBH_{3.75}F_{0.25}$ ($a = 3$) as a function of arbitrary identification numbers for the complete set of 81 possible configurations, divided in families according to the number of F on the same/different tetrahedra for the "locality principle" validation.

cation, by symmetry equivalence, of all the possible configurations obtained at the same F content; (ii) after full geometry optimization, to compute vibrational and thermodynamical properties of the Li–B–H–F structures; (iii) to calculate ΔH, ΔS and ΔG for the reaction

$$(1 - a/16)\mathrm{LiBH_4} + (a/16)\mathrm{LiBH_4} \rightarrow (1/4)\mathrm{Li_4B_4H_{16-a}F_a} \quad (1)$$

at $T = 298$ K and $p = 0.1013250$ MPa, where a represents the number of F ions which substitute H inside the unit cell ($0 \le a \le 16$).

To classify all the possible configurations for $1 \le a \le 15$ by symmetry, in order to run the expensive quantum-mechanical calculations for the irreducible ones only, we adopted a combinatorial mapping for solid solution recently implemented in the CRYSTAL09 code [28]. For instance, for $a = 1$, that is one H substituted with F out of 16 in the u.c., 16 configurations are possible, but only 3 of them are not symmetry equivalent and should be computed by quantum-mechanical calculation. Table 2 shows, for a ranging from 1 to 8 (the latter means half H in the u.c. substituted by F), that the total number of configurations increases very rapidly and becomes 12870 for $a = 8$, which reduces thanks to symmetry equivalence to 1720 classes. In principle, it is sufficient to perform quantum-mechanical calculations on these 1720 structures, which are however too many to be feasible with our computational facilities. Only for low a values (1 or 2) the number of classes is within reach, while for $a > 2$ it becomes too demanding. The crucial point was to find a way to filter out the less relevant (high energy) structures from the most stable ones within a given pool of classes without actually performing, for all of them, the expensive quantum-mechanical calculation.

Fig. 2 describes three examples of structures obeying to an assumption that we called the "locality principle". It states that those configurations where F ions substitute H on the same tetrahedron (T_d in Fig. 2) are the most stable ones, *i.e.* their quantum-mechanical total energy is the smallest. We have tested this handy rule at first on a limited number of configurations for several a values. In Fig. 2, structures and relative electronic energy data are displayed for some fully optimized models with $a = 2$, 3 and 4. For all cases the "locality principle" is followed, as the data show that the higher the number of F atoms for a given tetrahedron, the higher the stability of the resulting structure. This means, for instance, that the least stable configuration sports all F atoms on different tetrahedral units. For the $a = 2$ case, the electronic energy difference of about 50 kJ mol^{-1} per formula unit allows us to focus only on structures with 2F on the same tetrahedron. For $a = 4$, the differences in relative stability are smaller as other aspects also matter, such as the geometry optimization process or the F–F distance inside the unit cell.

To verify the validity of the "locality principle", we have explicitly computed the quantum-mechanical energies for all the 81 configurations of $a = 3$ case, *i.e.* for the $LiBH_{3.25}F_{0.75}$ formula unit composition (see Table 2, third row). Then, we have calculated ΔH values at $T = 298$ K for the reaction

$$(13/16)\mathrm{LiBH_4} + (3/16)\mathrm{LiBF_4} \rightarrow (1/4)\mathrm{Li_4B_4H_{13}F_3} \quad (2)$$

and have analyzed the resulting data in terms of the "locality principle".

Fig. 3 reports ΔH values as a function of arbitrary identification numbers for the 81 optimized structures. Results are divided in three families: (i) 3F on the same T_d; (ii) 2F + 1F on two different T_d and (iii) 1F + 1F + 1F on three different tetrahedra. The first family (3F on T_d) contains three structures, the most stable with $\Delta H = 6.9$ kJ mol^{-1} f.u. and the other two within 14.4 and 14.8 kJ mol^{-1} f.u. The second and third families (2F + 1F and 1F + 1F + 1F) are characterized by ΔH values around 25 and 33 kJ mol^{-1} f.u., respectively. A small number of outliers are present. The $\Delta H = 8.0$ kJ mol^{-1} f.u. for the reaction (2) was computed as the Boltzmann weighted average at 298 K of the 81 ΔH values of Fig. 3, according to:

$$\Delta H_{\mathrm{av}}(T) = \sum_c P_c(T)\, \Delta H_c \quad (3)$$

where ΔH_{av} represents the averaged enthalpy, c ranges from 1 to the total number of non equivalent classes with the same number of H/F substitutions inside the u.c. and the Boltzmann weight $P_c(T)$ is computed as

$$P_c(T) = \frac{W_c \exp(-(\Delta H_0)/RT)}{\sum_c W_c \exp(-(\Delta H_0)_c/RT)} \quad (4)$$

with W_c being the number of symmetry equivalent configurations for each class c and $(\Delta H_0)_c$ calculated adding the zero-point energy correction (ZPE) to the electronic energy.

Obviously, the Boltzmann average only favours the very stable structures which contribute to the averaged ΔH. On the basis of these results for $a = 3$, we have assumed the "locality principle" to hold true for all the compositions a ranging from 1 to 15 H substituted by F in the u.c.

Fig. 4 shows the Boltzmann weighted ΔH values derived from the quantum-mechanical calculations for the general reaction (1). The quantum-mechanical data of mixed compounds (squares in

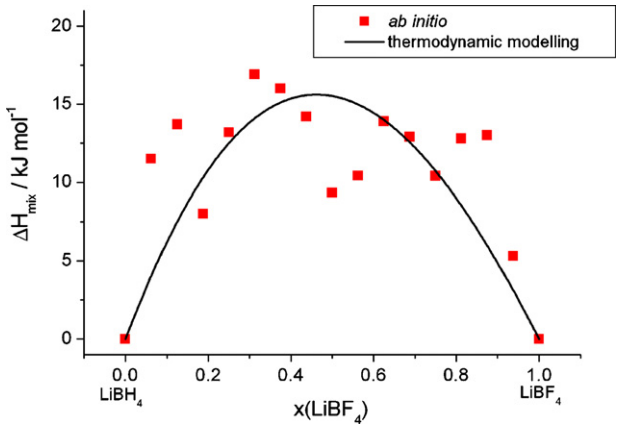

Fig. 4. Calculated excess enthalpy of mixing as a function of composition in the orthorhombic $LiBH_4$–$LiBF_4$ solid solution at 298 K and 1 bar (line) in comparison with the results from first principles calculations (squares).

the graph of Fig. 4) were used to derive the ΔH curve by thermodynamic modelling, using Thermocalc [25] according to:

$$\Delta H_{\text{mix}} = x(1-x)[L_0 + L_1(2x-1)] \quad (5)$$

where x is the molar fraction of $LiBF_4$ and $L_0 = 62438\,\text{J mol}^{-1}$ and $L_1 = -9750\,\text{J mol}^{-1}$ are the interaction parameters. At room temperature, changes in enthalpy are positive for all compositions, from the pure hydride to the pure fluoride, indicating that solubility is thermodynamically disfavoured.

4. Conclusions

The formation of solid solutions between orthorhombic $LiBH_4$ and orthorhombic $LiBF_4$ has been investigated by means of quantum-mechanical periodic calculation based on DFT (PBE functional) and local Gaussian basis set. We have shown that a "locality principle" holds true, which allows us to select a limited number of $LiB(H,F)_4$ structures to perform full quantum-mechanics calculations and derive their thermodynamical properties. Positive values of ΔH for the mixing reaction at room temperature indicate that the formation of mixed compounds is not favoured at any H/F ratio. Further work should deal with the substitution in the pure hydride of different anions, such as Chlorine, as well as other metal borohydrides.

Acknowledgment

Financial support from the European Union under FP7 (FLYHY project, grant agreement 226943) is thankfully acknowledged.

References

[1] L. Schlapbach, A. Züttel, Nature 414 (2001) 353–358.
[2] S. Orimo, Y. Nakamori, G. Kitahara, K. Miwa, N. Ohba, S. Towata, A. Züttel, J. Alloys Compd. 404–406 (2005) 427–430.
[3] A. Züttel, A. Remhof, A. Borgschulte, O. Friedrichs, Phil. Trans. R. Soc. A 368 (2010) 3329–3342.
[4] J. Yang, A. Sudik, C. Wolverton, J. Phys. Chem. C 111 (2007) 19134–19140.
[5] D. Ravnsbæk, Y. Filinchuk, Y. Cerenius, H.J. Jakobsen, F. Besenbacher, J. Skibsted, T.R. Jensen, Angew. Chem. Int. Ed. 48 (2009) 6659–6663.
[6] T.K. Nielsen, U. Boesenberg, R. Gosalawit, M. Dornheim, Y. Cerenius, F. Besenbacher, T.R. Jensen, ACS Nano 4 (2010) 3903–3908.
[7] H.W. Brinks, A. Fossdal, B.C. Hauback, J. Phys. Chem. C 112 (2008) 5658–5661.
[8] N. Eigen, U. Bösenberg, J. Bellosta von Colbe, T.R. Jensen, Y. Cerenius, M. Dornheim, T. Klassen, R. Bormann, J. Alloys Compd. 477 (2009) 76–80.
[9] H. Oguchi, M. Matsuo, J.S. Hummelshøj, T. Vegge, J.K. Nørskov, T. Sato, Y. Miura, H. Takamura, H. Maekawa, S. Orimo, Appl. Phys. Lett. 94 (2009) 141912.
[10] F.J. Torres, P. Ugliengo, B. Civalleri, A. Terentyev, C. Pisani, Int. J. Hydrogen. Energy 33 (2008) 746–754.
[11] J.S. Hummelshøj, D.D. Landis, J. Voss, T. Jiang, A. Tekin, N. Bork, M. Dułak, J.J. Mortensen, L. Adamska, J. Andersin, J.D. Baran, G.D. Barmparis, F. Bell, A.L. Bezanilla, J. Bjork, M.E. Björketun, F. Bleken, F. Buchter, M. Bürkle, P.D. Burton, B.B. Buus, A. Calborean, F. Calle-Vallejo, S. Casolo, B.D. Chandler, D.H. Chi, I. Czekaj, S. Datta, A. Datye, A. DeLaRiva, V. Despoja, S. Dobrin, M. Engelund, L. Ferrighi, P. Frondelius, Q. Fu, A. Fuentes, J. Fürst, A. García-Fuente, J. Gavnholt, R. Goeke, S. Gudmundsdottir, K.D. Hammond, H.A. Hansen, D. Hibbitts, J.E. Hobi, J.G. Howalt, S.L. Hruby, A. Huth, L. Isaeva, J. Jelic, I.J.T. Jensen, K.A. Kacprzak, A. Kelkkanen, D. Kelsey, D.S. Kesanakurthi, J. Kleis, P.J. Klüpfel, I. Konstantinov, R. Korytar, P. Koskinen, C. Krishna, E. Kunkes, A.H. Larsen, J.M.G. Lastra, H. Lin, O. Lopez-Acevedo, M. Mantega, J.I. Martínez, I.N. Mesa, D.J. Mowbray, J.S.G. Mýrdal, Y. Natanzon, A. Nistor, T. Olsen, H. Park, L.S. Pedroza, V. Petzold, C. Plaisance, J.A. Rasmussen, H. Ren, M. Rizzi, A.S. Ronco, C. Rostgaard, S. Saadi, L.A. Salguero, E.J.G. Santos, A.L. Schoenhalz, J. Shen, M. Smedemand, O.J. Stausholm-Møller, M. Stibius, M. Strange, H.B. Su, B. Temel, A. Toftelund, V. Tripkovic, M. Vanin, V. Viswanathan, A. Vojvodic, S. Wang, J. Wellendorff, K.S. Thygesen, J. Rossmeisl, T. Bligaard, K.W. Jacobsen, J.K. Nørskov, T. Vegge, J. Chem. Phys. 131 (2009) 014101.
[12] H. Hagemann, Y. Filinchuk, D. Chernyshov, W. van Beek, Phase Transit. 82 (2009) 344–355.
[13] L.-C. Yin, P. Wang, X.-D. Kang, C.-H. Sun, H.-M. Cheng, Phys. Chem. Chem. Phys. 9 (2007) 1499–1502.
[14] L. Yin, P. Wang, Z. Fang, H. Cheng, Chem. Phys. Lett. 450 (2008) 318–321.
[15] J.Y. Lee, Y.-S. Lee, J.-Y. Suha, J.-H. Shim, Y.W. Cho, J. Alloys Compd. (2010), doi:10.1016/j.jallcom.2010.07.051.
[16] J.P. Perdew, K. Burke, M. Ernzerhof, Phys. Rev. Lett. 77 (1996) 3865–3868.
[17] R. Dovesi, R. Orlando, B. Civalleri, C. Roetti, V.R. Saunders, C.M. Zicovich-Wilson, Z. Kristallogr. 220 (2005) 571–573.
[18] R. Dovesi, V.R. Saunders, C. Roetti, R. Orlando, C.M. Zicovich-Wilson, F. Pascale, B. Civalleri, K. Doll, N.M. Harrison, I.J. Bush, P. D'Arco, M. Llunell, CRYSTAL2009 User's Manual; University of Torino, Torino, 2009, http://www.crystal.unito.it.
[19] M. Merawa, P. Labeguerie, P. Ugliengo, K. Doll, R. Dovesi, Phys. Lett. 387 (2004) 453–459.
[20] R. Orlando, R. Dovesi, C. Roetti, J. Phys.-Condes. Matter 38 (1990) 7769–7789.
[21] C. Gatti, V.R. Saunders, C. Roetti, J. Chem. Phys. 101 (1994) 10686–10696.
[22] R. Nada, C.R.A. Catlow, C. Pisani, R. Orlando, Modell. Simul. Mater. Sci. Eng. 1 (1993) 165–187.
[23] F. Pascale, C.M. Zicovich-Wilson, F.L. Gejo, B. Civalleri, R. Orlando, R. Dovesi, J. Comput. Chem. 25 (2004) 888–897.
[24] C.M. Zicovich-Wilson, F.J. Torres, F. Pascale, L. Valenzano, R. Orlando, R. Dovesi, Comput. Chem. 29 (2008) 2268–2278.
[25] Thermo-Calc Software, http://www.thermocalc.com/.
[26] M.R. Hartman, J.J. Rush, T.J. Udovic, R.C.j. Bowman, S.J. Hwang, J. Solid State Chem. 180 (2007) 1298–1305.
[27] K. Matsumoto, R. Hagiwara, Z. Mazej, E. Goreshnik, B. Zemva, J. Phys. Chem. B 110 (2006) 2138–2141.
[28] A. Meyer, P. D'Arco, R. Orlando, R. Dovesi, J. Phys. Chem. C 113 (2009) 14507–14511.